

Effect of oxygen-doping on $\text{Bi}_2\text{Sr}_2\text{Ca}_2\text{Cu}_3\text{O}_{10+\delta}$ vortex matter: Crossover from electromagnetic to Josephson interlayer coupling

A. Piriou,* Y. Fasano, E. Giannini, and Ø. Fischer

Département de Physique de la Matière Condensée, Université de Genève,

24 Quai Ernest-Ansermet, 1211 Geneva, Switzerland

(Dated: October 30, 2018)

Abstract

We study the effect of oxygen-doping on the critical temperature, T_c , the vortex matter phase diagram and the nature of the coupling mechanism between the Cu-O layers in the three-layer $\text{Bi}_2\text{Sr}_2\text{Ca}_2\text{Cu}_3\text{O}_{10+\delta}$ (Bi-2223) compound. Contrary to previous reports, in the overdoped (OD) regime we do find a variation of T_c with increasing the oxygen partial-pressure of the post-annealing treatment. This variation is less significant than in the bi-layer parental compound $\text{Bi}_2\text{Sr}_2\text{CaCu}_2\text{O}_{10+\delta}$ (Bi-2212) and does not follow the universal T_c vs. δ relation. Magnetic measurements reveal that increasing δ enlarges the field and temperature stability of the Bragg glass phase. These findings imply that the interlayer coupling between Cu-O layers enhances with δ . The anisotropy parameter estimated from directional first-penetration field measurements monotonously decreases from 50 in the underdoped (UD) to 15 in the OD regimes. However, the in-plane penetration depth presents a boomerang-like behaviour with δ , reaching its minimum value close to optimal doping. These two facts lead to a crossover from a Josephson(OD) to electromagnetic(UD)-dominated coupling of adjacent Cu-O layers in the vicinity of optimal doping.

PACS numbers: 74.72.Hs, 74.62.Dh, 74.25.Dw, 74.25.Ha

Keywords: Bi-2223, oxygen-doping, Cu-O layers coupling mechanism, vortex phase diagram

*Electronic address: Alexandre.Piriou@physics.unige.ch

Introduction

Understanding the extremely anisotropic electronic and magnetic properties of layered cuprates requires to unveil the nature of the coupling mechanism between the superconducting Cu-O layers. In these materials these layers are composed of a stack of Cu-O planes. The interlayer coupling between adjacent Cu-O layers is produced by Josephson tunnelling and by electromagnetic interactions between the supercurrents lying in the layers [1, 2]. The family of Bi-based compounds presents a weak interlayer coupling between the Cu-O layers [3] resulting in both terms being comparable. The possibility of the electromagnetic interaction being dominant over the Josephson one was thoroughly studied [3, 4, 5] for the bi-layer $\text{Bi}_2\text{Sr}_2\text{CaCu}_2\text{O}_{8+\delta}$ (Bi-2212) compound which presents one of the weakest interlayer coupling among cuprates [3]. In this work we address this issue in the less studied three-layer $\text{Bi}_2\text{Sr}_2\text{Ca}_2\text{Cu}_3\text{O}_{10+\delta}$ (Bi-2223) material by tuning the oxygen concentration in a single sample. Such studies in this compound are lacking due to the difficulty in obtaining pure and high-quality macroscopic crystals [6] for reliable magnetic measurements. This compound presents the highest critical temperature at optimal doping (OPT) among the Bi-based cuprates, $T_c^{\text{OPT}} = 110.5$ K.

The crystal structure of Bi-2223 is composed of insulating (blocking) layers intercalating in the c -axis direction with superconducting Cu-O layers. The spacing between the layers, formed by three Cu-O planes, is $s = 18$ Å for optimally-doped samples [7]. The interlayer coupling is inversely proportional to the electronic anisotropy, $\gamma = \sqrt{m_c/m_{ab}}$, given by the ratio between the effective masses in the c -axis and in the ab -plane [1]. As mentioned, this coupling is produced by two different mechanisms. The first, the Josephson coupling, consists of the hole-tunnelling from one Cu-O layer to the adjacent, through the blocking layer. This mechanism is dominant when $s\gamma < \lambda_{ab}(0)$ [2], where $\lambda_{ab}(0)$ is the in-plane penetration depth. The second mechanism arises from the electromagnetic interaction between the supercurrents located in adjacent Cu-O layers and is, on the contrary, dominant when $s\gamma > \lambda_{ab}(0)$ [2]. The relevance of these two mechanisms depends on the hole-carrier concentration and on the degree of charge-transfer between the Cu-O layers. One way to modify these magnitudes is to over-dope (OD) or under-dope (UD) with respect to the optimal oxygen content ($\delta = \delta_{OPT}$). Extra oxygen atoms will occupy vacancies in the blocking layers.

Oxygen-doping produces quantitative changes in the vortex phase diagram. Flux lines

in the extremely anisotropic Bi-based cuprates are composed of a stack of poorly-coupled pancake vortices located in the Cu-O layers [1]. This weak coupling leads to the liquid vortex phase spanning a considerable fraction of the $H - T$ phase diagram [8]. On cooling at low magnetic fields vortex matter undergoes a first-order solidification transition at T_m [8, 9]. On further cooling the vortex magnetic response becomes irreversible since pinning sets-in at a temperature $T_{IL}(H) \lesssim T_m(H)$, the so-called irreversibility line. The phase stable at low temperatures, the Bragg glass [10, 11], exhibits quasi-crystalline order. With increasing magnetic field the vortex structure transforms into a topologically disordered glass [12] through a first-order phase transition known as the second-peak line, H_{SP} [13, 14]. The vortex glass melts with increasing temperature through a second-order phase transition [15]. In the case of Bi-2212, the Bragg glass phase spans up to higher temperatures and fields with increasing oxygen concentration [5, 14, 16], which is consistent with a decrease of γ with δ . Introducing extra oxygen atoms also affects the pinning potential landscape [17]. Nevertheless, changes in the vortex phase diagram provide information on the evolution of the interlayer coupling with doping. In this work we report on the doping-dependence of the critical current density, $J_c(T, H)$, and on the evolution of $H_{SP}(T)$, $H_{IL}(T)$, and $T_{OD}(H)$, the zero-dimensional pinning temperature at which pancake vortices of every Cu-O layer are individually pinned. We find that changes in the oxygen-doping level of Bi-2223 affect the vortex phase diagram in a similar manner than in Bi-2212. However, since Bi-2223 is three times less anisotropic than Bi-2212, significant differences are also detected.

In the case of the bi-layer compound, increasing the oxygen concentration results in a monotonous reduction of γ [3, 5], and of the c -axis lattice parameter [5], and consequently s . However, $\lambda_{ab}(0)$ evolves in a non-monotonous way with δ , being minimum in the slightly OD regime [4, 5, 18, 19]. Therefore, given that in Bi-based compounds $s\gamma \sim \lambda_{ab}$, a crossover from electromagnetic to Josephson-dominated coupling is quite likely when decreasing δ . Evidence of this crossover was indeed reported in the case of Bi-2212 [5]. Nevertheless, as the anisotropy of Bi-2223 is smaller than that of Bi-2212, in the three-layer compound the Josephson coupling might be dominant in a wider δ region. In this work we address the question whether a crossover from Josephson to electromagnetic coupling is plausible in Bi-2223. We find that when decreasing δ , on top of increasing the magnitude of the electronic anisotropy, this crossover takes place in the vicinity of optimal doping.

Crystal-growth and oxygen-doping

Bi-2223 and Bi-2212 crystals were grown by means of the travelling-solvent floating-zone method as described in Ref. [6]. The structural and superconducting properties of the crystals used in this work are reported in Refs. [7, 20]. X-Ray diffraction measurements have revealed the phase purity and the high crystalline order of our samples. In the case of the Bi-2223 samples its quality has allowed the refinement of the crystal structure from single-crystal X-ray diffraction data [7]. Electrical resistivity and magnetic susceptibility measurements reveal a single and sharp superconducting transition (examples are shown in the insert of Fig. 1). Considering the measurements resolution, these results indicates that, if present, Bi-2212 intergrowths represent less than 1 % of the volume of the samples.

In order to tune and to homogenize the hole concentration the crystals were annealed during 10 days at 500°C, under various oxygen partial pressures, $p(O_2)$. In Fig. 1 we compare the dependence of T_c on $p(O_2)$ for both Bi-2212 and Bi-2223 crystals. Every point results from an average over at least 10 samples annealed in the same conditions. At every $p(O_2)$ value, the critical temperature and the transition width are the same within the error, as measured by means of AC susceptibility and DC magnetization. The reliability of these results allows us to consider the critical temperature as a measure of the macroscopic oxygen content. The transition temperature T_c is taken as the temperature at which $\partial\chi'/\partial T$ and $\partial M/\partial T$ exhibit a peak. The transition widths are estimated as the FWHM of these peaks and range from 0.6 to 2 K. This is an indication that in our crystals the oxygen distribution is rather homogeneous.

In the case of Bi-2212 samples the T_c vs. $p(O_2)$ data are in quantitative agreement with the existing literature [3] and do not deserve any further comment. However, the results for Bi-2223 are in qualitative disagreement with previous reports [21, 22]. As in the case of these works, our OPT Bi-2223 samples, with $T_c = (110.5 \pm 0.5)$ K, are obtained at quite a high partial pressure, $p(O_2^{OPT}) = 20$ bar. For higher annealing pressures the samples become overdoped. Fig. 1 shows that T_c does change in the OD regime, decreasing from (110.5 ± 0.5) to $(107.0 + 0.5)$ K. This is in contrast with the works of Fujii *et al.* [21] and Liang *et al.* [22] which report a T_c vs. $p(O_2)$ plateau in the OD regime. The authors [21, 22] claim that this plateau results from a different doping level of the inner and outer planes of the Cu-O layers, the inner being less doped [23]. This interpretation is based on a theoretical model

that assumes a strong interlayer coupling [24].

In spite of the inner and outer Cu-O planes having a different doping level [23], other factors might be at the origin of the T_c -plateau reported in Refs. [21, 22]. As a matter of fact, an inhomogeneous oxygen distribution throughout the sample can be responsible for an apparent insensitivity of T_c to oxygen doping. An inhomogeneous oxygen distribution is also compatible with the detected decrease of the c -axis lattice parameter [21] and the enhancement of the vortex irreversibility field [22] with increasing δ . Crystals exhibiting a broader superconducting transition than ours, like the ones reported in Refs. [21, 22], might present an inhomogeneous oxygen spatial-distribution. In such crystals the onset of the superconducting transition would be determined by the OPT domains, whereas the shift of the x-ray reflections and the enhancement of $H_{IL}(T)$ would be dominated by the OD ones. The narrower superconducting transitions measured in our crystals indicate that their spatial oxygen distribution is more homogeneous and as a consequence the detected decrease of T_c in the OD regime is not hidden by inhomogeneities of the samples.

The most striking result of Fig. 1 is that a larger oxygen partial-pressure is required in order to reach optimal doping in Bi-2223 than in Bi-2212. Our results for Bi-2212 samples are in agreement with the established bell-shaped dependence of T_c with oxygen concentration [25, 26, 27], see fits of Fig. 1. On the contrary, in the case of Bi-2223 the curve resulting from adjusting the UD data with the universal T_c vs. doping ($p(O_2)$) relation [25, 26] does not fit the points in the OD regime. Seminal works on three-layer cuprates already reported that T_c follows the universal law in the UD region [26, 28]. Our results in Bi-2223 confirm this and also indicate that in the OD regime of three-layer compounds the universal law [25, 26] is not fulfilled as in the case of single- and bi-layer cuprates. This phenomenology can be related to the different doping level of the outer and inner Cu-O planes.

Doping-dependence of the vortex phase diagram

As mentioned, to study the effect of hole-doping on the vortex phase diagram of Bi-2223 the oxygen content was tuned in the same sample. The results presented in this section correspond to doping levels in the UD ($T_c = (100 \pm 2)$ K), OPT ($T_c = (110.5 \pm 0.5)$ K) and OD ($T_c = (107.0 \pm 0.5)$ K) regimes.

The vortex phase diagram was studied by means of bulk magnetic measurements using

a Quantum-design SQUID magnetometer and a PPMS measurement system. In particular, we report on the evolution of the irreversibility line, $H_{\text{IL}}(T)$, the order-disorder $H_{\text{SP}}(T)$ transition line, associated with a peak in the critical current [13, 14]; and the zero-dimensional pinning line T_{0D} [29, 30]. These lines were obtained from magnetization *vs.* temperature measurements, $M(T)$, following zero-field- (ZFC) and field-cooling (FC) paths, and from hysteresis magnetization loops, $M(H)$. For these measurements the field was applied out-of-plane, i.e. $H \parallel c$ -axis. The typical field and temperature sweep-rates in $M(H)$ and $M(T)$ measurements were of 10^{-2} Gauss/sec and 10^{-3} K/sec, respectively. Figure 2 presents typical magnetization data for doping levels corresponding to the UD, OPT and OD regimes. The superconducting transition in each case is shown in the insert of Fig. 1.

The onset of the irreversible magnetic response was obtained from field- and zero-field-cooling $M(T)$ curves as the kink detected at a temperature $T_{\text{IL}}(H)$ higher than that where both branches merge [31], see Fig. 2 (b). The hole-doping dependence of the irreversibility line is shown in the H *vs.* T/T_c phase diagram of Fig. 3. At any reduced temperature, the irreversibility field is enhanced with increasing the oxygen-doping level. The evolution of $H_{\text{IL}}(T)$ with doping for the bi-layer compound [5] and data previously reported for Bi-2223 [22, 32] follow the same trend.

The enlargement of the solid vortex phase is consistent with an enhancement of the interlayer coupling by increasing oxygen concentration, and consequently a reduction of the anisotropy parameter. Theoretical studies indicate that the melting [33] and decoupling [34] lines shift towards higher temperatures as soon as a small Josephson coupling between the layers is considered on top of electromagnetic interactions. In the case of platelet-like samples, such as the ones studied in this work, for Bi-2212 at low fields the irreversibility coincides with the melting and decoupling lines [8, 30]. Therefore, the enhanced stability of the solid vortex phase shown in Fig. 3 can be associated with an increasingly relevant role of the Josephson coupling when raising the doping level. This is quite likely since $s\gamma \gtrsim \lambda_{\text{ab}}$ for the OPT regime of Bi-2223. This issue will be further discussed in the next section.

The transition line $H_{\text{SP}}(T)$ is manifested as a peak-valley structure in $M(H)$ curves, as evident in the magnetization loops of Fig. 2 (a). We considered $H_{\text{SP}}(T)$ to be the field at which M has an inflection point between the peak and the valley (indicated by arrows in the figure), averaging the values for the two branches of the loop. The phase diagram of Fig. 3 shows that the second-peak line is roughly temperature-independent, as also found

in Bi-2212 [5, 14, 30]. Theoretical works considering the $H_{\text{SP}}(T)$ line as an order-disorder phase transition between the low-field Bragg glass and the high-field vortex glass [11, 35] estimate $H_{\text{SP}}(T)$ as the field where the elastic energy of the vortex structure equals the pinning energy. These two energy terms depend on the penetration depth, coherence length and anisotropy of the material, as well as on the pinning parameter [11]. Therefore, the temperature evolution of H_{SP} is determined by the temperature dependence of λ_{ab} and ξ_{ab} [36]. Figure 3 shows that for the three doping levels studied H_{SP} is detected only in the temperature range $0.2 \lesssim T/T_c \lesssim 0.55$. Considering the two-fluid expression for λ_{ab} and ξ_{ab} [1], in this temperature range both magnitudes vary within 3%. This minimal variation and the important anisotropy [36] of the material are responsible for the observed roughly temperature-independent H_{SP} .

The temperature-averaged H_{SP} increases with doping: (340 ± 20) Oe for the UD, (630 ± 40) Oe for the OPT and (1040 ± 60) Oe for the OD regimes. The same qualitative behavior was reported in Bi-2212 [5, 14, 16] and other cuprates [37]. The evolution of $H_{\text{SP}}(T)$ with doping is consistent with an enhancement of coupling between the Cu-O planes with increasing oxygen concentration, as also suggested by the doping dependence of $H_{\text{IL}}(T)$ [2]. This point will be further discussed in the next section.

The zero-dimensional pinning line, T_{0D} , that separates the regime where individual pancake vortices are pinned ($T < T_{\text{0D}}$) from that where vortex lines are pinned individually, can be obtained from critical current density *vs.* temperature curves $J_c(T)$ at a given magnetic field [38]. In the low-temperature zero-dimensional pinning regime not only the vortex-pinning interaction overcomes the vortex-vortex interaction but also pancake vortices belonging to the same vortex but to different Cu-O layers are pinned individually [1]. Therefore at temperatures $T < T_{\text{0D}}$ the critical current should be field independent at low fields. This is a consequence of the *c*-axis Larkin correlation length, $L_c^c \sim (r_p/\gamma)(J_0/J_c)^{1/2}$ [39], becoming smaller than the Cu-O layers spacing s [1]. In the last expression $r_p \sim \xi$ is the typical pinning range and $J_0 = 4c\Phi_0/12\sqrt{3}\pi\lambda_{\text{ab}}^2\xi_{\text{ab}}$ is the depairing current density. Therefore $T_{\text{0D}}(T)$ can be estimated as the temperature at which $J_c(T)$ presents a kink and a steeper increase in the low-temperature region [38]. In this work we consider the same criterion to estimate T_{0D} .

The critical current is obtained from magnetization loops measured at different temperatures as the examples shown in Fig. 2 (a). Considering the Bean model [40], at a given

temperature $J_c(T, H) \sim (3c/2R)\Delta M(T, H)$, where $\Delta M(T, H)$ is the separation between the two branches of the magnetization loop at a field H , c is the speed of light and R is the radius of an equivalent cylindrical sample [40]. Figure 4 reveals that the critical current of Bi-2223 is one order of magnitude larger than that of Bi-2212 [38] at similar reduced temperatures and fields. From this figure it is also evident that at low temperatures the critical current is field-independent at low fields, which is a fingerprint of the individual pinning regime (either of flux lines or of individual pancakes). The insert of Fig. 4 shows typical $J_c(T/T_c)$ curves at an applied field of 40 Oe for the UD, OPT and OD regimes. The kink in critical current identified as T_{0D} is indicated with arrows. Considering that for the OPT regime of Bi-2223 $\xi \sim 10 \text{ \AA}$ [41], $J_0 = 6.15 \cdot 10^8 \text{ A/cm}^2$, $\gamma = 27 \pm 4$ (see data shown in the next section), and $J_c(T_{0D}) = 1.81 \cdot 10^5 \text{ A/cm}^2$, a value of $L_c^c = 24 - 18$, close to s is estimated at $T = T_{0D}$. Similar values for L_c^c are obtained for the UD and OD regimes.

For every doping level the zero-dimensional-pinning line is roughly field-independent, as also found in Bi-2212 [5, 30]. Since T_{0D} is the temperature at which the individual pinning of pancake vortices sets in, then $J_c(T)$ is almost field-independent for $T \leq T_{0D}$. Therefore, $L_c^c \sim (r_p/\gamma)(J_0/J_c(T_{0D}))^{1/2}$ equals the Cu-O layers spacing at a temperature T_{0D} that is roughly field-independent. The location of T_{0D} is however doping dependent. The zero-dimensional pinning line is placed at $(18.5 \pm 0.5) \text{ K}$ for the UD, $(24 \pm 1) \text{ K}$ for the OPT and $(25 \pm 1) \text{ K}$ for the OD regimes. A study on the OPT and OD regime of Bi-2212 samples reports that T_{0D} does not significantly change with doping [38]. However, as the magnitude of $J_c(T_{0D})$ is in direct relation with T_{0D} (see Fig. 4), if γ decreases then, in order to fulfill $L_c^c = s$, $J_c(T_{0D})$ and therefore T_{0D} have to increase. The difference between our results in Bi-2223 and those reported for Bi-2212 [38] might originate in the fact that in the latter study the anisotropy changes are of the order of 30% whereas in our case they are 5 times greater than this value (see the next section for detailed data in this respect). Therefore, an increment of the zero-dimensional temperature with doping is in agreement with the enhancement of interlayer coupling suggested by the doping evolution of $H_{IL}(T)$ and $H_{SP}(T)$.

One interesting result of the vortex phase diagrams shown in Fig. 3 is that for $T < T_{0D}$ the order-disorder second peak line is no longer detected within our experimental resolution. Similar findings were observed in Bi-2212 samples [30, 38]. The vortex glass phase located at $H > H_{SP}$ presents no vortex phase correlation in the c direction [30], whereas the zero-dimensional pinning region is correlated in the ab plane as well as in the perpendicular

direction [38]. Therefore, the suppression of the vortex phase correlation along the c direction takes place only when L_c^c exceeds the spacing between the Cu-O layers. This suggests that the establishment of a zero-dimensional pinning regime inhibits the vortex structure instability associated with the order-disorder phase transition detected at $T > T_{0D}$.

In summary, the doping dependence of the transition lines $H_{IL}(T)$ and $H_{SP}(T)$ and the crossover temperature T_{0D} are in agreement with an enhancement of the coupling between Cu-O layers with increasing doping. The decrease of γ on overdoping suggested by the results presented in this section implies that the Josephson coupling term between adjacent layers becomes increasingly relevant. Therefore, the scenario of a crossover from electromagnetic(UD) to Josephson(OD)-dominated interlayer coupling is quite likely. However, a possible non-monotonous evolution of λ_{ab} with doping has to be explored in order to differentiate between this scenario and the situation where the interlayer coupling increases but continues to be electromagnetic in nature when overdoping.

Crossover from electromagnetic to Josephson coupling when overdoping

In order to study the nature of the coupling between the Cu-O layers of Bi-2223 as a function of doping we quantitatively compared the characteristic lengths $s\gamma$ and $\lambda_{ab}(0)$. In the case of Bi-2212 a crossover from electromagnetic ($s\gamma > \lambda_{ab}$) to Josephson($s\gamma < \lambda_{ab}$)-dominated interlayer coupling takes place slightly above the OPT regime (for $T_c \sim 0.9T_c^{max}$) [5]. We study this possibility in the case of Bi-2223.

The in-plane penetration depth is extracted from measurements of the first penetration field with H applied perpendicular to the Cu-O planes, H_{c1}^\perp , for different temperatures in the range 35-60 K. The first penetration field was obtained from M vs. H loops where the magnetic relaxation at every field was measured during one hour. This was done in order to avoid the effect of surface and geometrical pinning barriers [42]. The effective first penetration field for the sample was considered as that where the magnetization shows a detectable relaxation, associated with the entrance of the first vortex. The effect of the demagnetizing factor of the sample estimated from the Meissner slope was considered in order to obtain H_{c1}^\perp . The value of $\lambda_{ab}(0)$ was obtained by fitting the temperature-dependent H_{c1}^\perp within the London model, $H_{c1}^\perp = (\Phi_0 / (4\pi\lambda_{ab}(T)^2) \ln(\lambda_{ab}(T)/\xi_{ab}(T)))$, and considering the two-fluid model expressions for $\lambda_{ab}(T)$ and $\xi_{ab}(T)$ [1]. The zero-temperature coherence length is

taken as $\xi(0) = 10 \text{ \AA}$, as suggested by Scanning Tunnelling Microscopy measurements of the superconducting density of states in the vicinity of a vortex [41].

The boomerang-like dependence of $\lambda_{ab}(0)$ with oxygen concentration is shown in Fig. 5: it decreases from the UD towards the OPT region and then substantially increases in the OD regime. This non-monotonic evolution is in agreement with results obtained in other cuprates [4, 19, 44]. It was originally proposed that this decrease of the superfluid density in the OD regime results from a substantial pair breaking in spite of the normal-state carrier concentration increasing when overdoping [19]. However, Scanning Tunnelling Microscopy data on several cuprates are at odds with this interpretation since the superconducting quasi-particle peaks sharpen on increasing doping [43]. Therefore, the origin of this phenomenon remains still as an open question.

The anisotropy parameter is estimated from the first penetration field for H applied perpendicular and parallel to the Cu-O planes since within the London approximation $\gamma = H_{c1}^{\perp}/H_{c1}^{\parallel}$ [1]. The values of H_{c1}^{\parallel} were measured by aligning the sample with a home-made rotation system that reduces the misalignment uncertainty to $\sim 0.5^{\circ}$. The effect of the demagnetizing factor was corrected from the Meissner slope, giving a value in accordance with the $D_{\parallel} \sim (1 - D_{\perp})/2$ relation found for platelet-like samples. The values of γ presented in the insert of Fig. 5 correspond to averaging results obtained at different temperatures ranging between 35 and 60 K. The error bar in the points represent the dispersion of values measured at different temperatures. The anisotropy parameter monotonically decreases with increasing oxygen concentration. This establish that the interlayer coupling is enhanced with increasing the oxygen concentration, as suggested by the results presented in the previous section. We estimate a value of $\gamma = (27 \pm 3)$ for the optimally doped sample, smaller than previously reported [45]. It is important to point out that our estimation is a result of measuring the first critical field at various temperatures whereas in Ref. [45] it was estimated from measurements at a single temperature.

The same evolution of the anisotropy parameter with oxygen-doping was found for Bi-2212, one of the most anisotropic cuprates. The insert of Fig. 5 compares the evolution of γ with T_c/T_c^{max} for the bi-layer and three-layer Bi-based compounds. Although the Bi-2212 data are roughly three times larger than the Bi-2223 ones, the variation of γ relative to γ^{OPT} is similar in both compounds. Therefore the coupling between the Cu-O layers of Bi-2223 is affected by oxygen-doping in a similar amount, relative to γ^{OPT} , than in Bi-2212.

Changes in the oxygen concentration affect the anisotropy parameter mostly because the number of carriers in the charge reservoir blocks varies, but also because the c -axis lattice parameter is slightly modified. Adding extra oxygen reduces the c -axis lattice parameter and therefore s [5]. In the case of Bi-2212 the overdoping-induced decrease of the c -axis lattice parameter was found to be of only $\sim 0.5\%$ [5]. This change is much smaller than the error we have in determining γ , and therefore in estimating $s\gamma$ we consider the value $s = 18 \text{ \AA}$ measured in OPT samples as the spacing between the Cu-O layers at all doping levels.

Another parameter that gives information on the nature of the interlayer coupling is the doping evolution of $\sqrt{\Phi_0/H_{SP}}$. In the case of the interlayer coupling being dominated by the electromagnetic term, $\sqrt{\Phi_0/H_{SP}} \propto \lambda_{ab}$ [2]. On the contrary, if the Josephson interaction dominates, $\sqrt{\Phi_0/H_{SP}} \propto s\gamma$ [2]. Figure 5 shows that $\sqrt{\Phi_0/H_{SP}}$ monotonously decreases with doping, and therefore significantly deviate from the evolution of λ_{ab} with doping in the OD regime.

To summarize, Fig. 5 shows a comparison of the characteristic lengthscales. In the OD regime, $s\gamma < \lambda_{ab}(0)$ and $\sqrt{\Phi_0/H_{SP}}$ does not follow the trend of $\lambda_{ab}(0)$ but rather that of $s\gamma$. These findings indicate that the Josephson interaction progressively dominates the interlayer coupling with increasing oxygen concentration from optimal doping. At the OPT regime $s\gamma$ becomes of the order of the in-plane penetration depth. Deep into the UD region $s\gamma$ slightly overcomes $\lambda_{ab}(0)$ and $\sqrt{\Phi_0/H_{SP}}$ follows the same trend than the penetration depth. These results constitute evidence that in the UD regime the interlayer coupling is dominated by the electromagnetic term. Therefore, with increasing doping from the UD to the OD regime not only the anisotropy decreases but the coupling between Cu-O layers changes in nature, presenting a crossover from a electromagnetic to a Josephson-dominated interaction. Although with our data the exact doping level at which this crossover takes place can not be accurately determined, it is evident that it occurs in the vicinity of the OPT regime.

I. CONCLUSIONS

We provide evidence that oxygen-doping in Bi-2223 crystals produces a non-negligible change of T_c in the OD regime, in contrast to previous claims [21, 22]. The changes in

T_c/T_c^{max} are non-symmetric with respect to optimal doping: in the OD regime they are greater than in the UD regime. Therefore, the evolution of T_c in the OD regime of Bi-2223 does not follow the universal relation with δ as found in many single- and bi-layer cuprates [25, 26].

Varying oxygen concentration affects the vortex matter phase diagram in a way that is consistent with an enhancement of the Cu-O interlayer coupling with increasing δ . Namely, the Bragg glass phase spans up to higher fields ($H_{SP}(T)$ increases) and temperatures ($T_{IL}(H)$ and $T_{0D}(H)$ increase) when overdoping. The evolution of $H_{IL}(T)$ and $H_{SP}(T)$ with doping is in agreement with results reported for the bi-layer parental compound [3, 5, 14]. In the case of the zero-dimensional pinning temperature we do detect an increase with δ contrary to reports on Bi-2212 [38]. This can be understood considering that in our work δ is varied in a much larger interval than in Ref. 38.

The suggested enhancement of the interlayer coupling with increasing δ is indisputably observed by the monotonous decrease of anisotropy with oxygen concentration. A comparison between the directly-measured magnitudes $s\gamma$, λ_{ab} , and $\sqrt{\Phi_0/H_{SP}}$ reveals that a crossover from Josephson(OD) to electromagnetic(UD)-dominated coupling takes place around optimal doping. This crossover originates from the non-monotonous behavior of λ_{ab} with δ . Therefore, the highly-anisotropic superconducting properties of UD Bi-2223 relies not only on a decrease of the magnitude of the Cu-O layer interaction but also in a change of the nature of its coupling mechanism.

The authors acknowledge G. Nieva for useful discussions and R. Lortz for assistance in the SQUID measurements. This work was supported by the MANEP National Center of Competence in Research of the Swiss National Science Foundation.

-
- [1] G. Blatter, M. V. Feigelman, V. B. Geshkenbein, A. I. Larkin and V. M. Vinokur, Rev. Mod. Phys. **66**, 1125 (1994).
 - [2] A. E. Koshelev, V.M. Vinokur, Phys. Rev. B **57**, 8026 (1998).
 - [3] K. Kishio, in *Coherence in High Temperature Superconductors*, edited by G. Deutscher and A. Revcolevschi (World Scientific, Singapore, 1996), p. 212, and references therein.
 - [4] G. Villard, D. Pelloquin, and A. Maignan, Phys. Rev. B **58** 15231 (1998).

- [5] V.F. Correa, E.E. Kaul, G. Nieva, Phys. Rev. B **63**, 172505 (2001).
- [6] E. Giannini, V. Garnier, R. Gladyshevskii and R. Flükiger, Supercond. Sci. Technol. **17**, 220 (2004).
- [7] E. Giannini, R. Gladyshevskii, N. Clayton, N. Musolino, V. Garnier, A. Piriou and R. Flükiger, Curr. App. Phys. **8**, 115 (2008).
- [8] H. Pastoriza, M. F. Goffman, A. Arribére and F. de la Cruz, Phys. Rev. Lett. **72**, 2951 (1994).
- [9] E. Zeldov, D. Majer, M. Konczykowski, V. B. Geshkenbein, V. M. Vinokur, and H. Shtrikman, Nature **375**, 373 (1995).
- [10] T. Nattermann, Phys. Rev. Lett. **64**, 2454(1990).
- [11] T. Giamarchi and P. L. Doussal, Phys. Rev. Lett. **72**, 1530 (1994).
- [12] D. S. Fisher, M. P. A. Fisher and D. A. Huse, Phys. Rev. B **43**, 130 (1991).
- [13] R. Cubbit, E. M. Forgan, G. Yang, S. L. Lee, D. McK. Paul, H. A. Mook, M. Yethiraj, P. H. Kes, T. W. Li, A. A. Menovsky, Z. Tarnawski, and K. Mortensen, Nature **365**, 407 (1993); E. Zeldov, D. Majer, M. Konczykowski, A. I. Larkin, V. M. Vinokur, V. B. Geshkenbein, N. Chikumoto and H. Shtrikman, Europhys. Lett. **30**, 367 (1995).
- [14] B. Khaykovich, E. Zeldov, D. Mayer, T. W. Li, P. H. Kes and M. Konczykowski, Phys. Rev. Lett. **76**, 2555 (1996).
- [15] B. Khaykovich, M. Konczykowski, E. Zeldov, R. A. Doyle, D. Majer, P. H. Kes, and T. W. Li, Phys. Rev. B **56**, R517 (1997).
- [16] K. Kishio *et al.*, in *Proceedings of the 7th International Workshop on Critical Currents in Superconductors*, edited by H. W. Weber (World Scientific, Singapore, 1994), p.339; C. Bernhard, C. Wenger, Ch. Niedermayer, D. M. Pooke, J. L. Tallon, Y. Kotaka, J. Shimoyama, K. Kishio, D. R. Noakes, C. E. Stronach, T. Sembiring and E. J. Ansaldo, Phys. Rev. B **52**, R7050 (1995); C. M. Aegerter, S.L. Lee, H. Keller, E.M. Forgan, S.H. Lloyd Phys. Rev. B **54**, R15661 (1996); T. Tamegai *et al.*, in *Proceedings of the 9th International Symposium on Superconductivity*, edited by S. Nakajima and M. Murakami (Springer-Verlag, Tokyo, 1997), p.621.
- [17] S. Ooi, T. Shibauchi and T. Tamegai, Physica C **302**, 339 (1998).
- [18] Y. J. Uemura, G. M. Luke, B. J. Sternlieb, J. H. Brewer, J. F. Carolan, W. N. Hardy, R. Kadono, J. R. Kempton, R. F. Kiefl, S. R. Kreitzman, P. Mulhern, T. M. Riseman, D. L. Williams, B. X. Yang, S. Uchida, H. Takagi, J. Gopalakrishnan, A. W. Sleight, M. A.

- Subramanian, C. L. Chien, M. Z. Cieplak, Gang Xiao, V. Y. Lee, B. W. Statt, C. E. Stronach, W. J. Kossler, and X. H. Yu, Phys. Rev. Lett. **62**, 2317 (1989); Y. J. Uemura, L. P. Le, G. M. Luke, B. J. Sternlieb, W. D. Wu, J. H. Brewer, T. M. Riseman, C. L. Seaman, M. B. Maple, M. Ishikawa, D. G. Hinks, J. D. Jorgensen, G. Saito, and H. Yamochi, Phys. Rev. Lett. **66**, 2665 (1991).
- [19] Ch. Niedermayer, C. Bernhard, U. Binniger, H. Glückler, J. L. Tallon, E. J. Ansaldo, and J. I. Budnick, Phys. Rev. Lett. **71**, 1764 (1993).
- [20] E. Giannini, N. Clayton, N. Musolino, R. Gladyshevskii, and R. Flükiger, in *Frontiers in Superconducting materials*, edited by A. Narlikar, (Springer-Verlag, London, 2005), p. 739.
- [21] T. Fujii, I. Terasaki, T. Watanabe and A. Matsuda, Phys. Rev. B **66**, 024507 (2002).
- [22] B. Liang, C. Bernhard, Th. Wolf and C. T. Lin, Supercond. Sci. Technol. **17**, 731 (2004).
- [23] A. Trokiner, L. Le Noc, J. Schneck, A. M. Pougnet, R. Mellet, J. Primot, H. Savary, Y. M. Gao and S. Aubry, Phys. Rev. B **44**, 2426 (1991).
- [24] S. A. Kivelson, Physica B **318**, 61 (2002).
- [25] C. Allgeier and J. S. Schilling, Physica C **168**, 499 (1990).
- [26] M. R. Presland, J. L. Tallon, R. G. Buckley, R. S. Liu and N. E. Flower, Physica C **176**, 95 (1991).
- [27] X. Zhao, X. Sun, X. Fan, W. Wu, X-G. Li, S. Guo and Z. Zhao, Physica C **307**, 265 (1998).
- [28] A. Schilling, H. R. Ott and F. hulliger, Physica C **157**, 144 (1989).
- [29] M. Nideröst, A. Suter, P. Visani, A. C. Mota and G. Blatter, Phys. Rev. B **53**, 9286 (1996).
- [30] M. F. Goffman, J. A. Herbsommer, F. de la Cruz, T. W. Li and P. H. Kes, Phys. Rev. B **57**, 3663 (1998).
- [31] A. Schilling, H. R. Ott and Th. Wolf, Phys. Rev. B **46**, 14253 (1992).
- [32] A. Piriou, Y. Fasano, E. Giannini and Ø. Fischer, Physica C **460-462**, 408 (2007).
- [33] G. Blatter, V. Geshkenbein, A. Larkin and H. Nordborg, Phys. Rev. B **54**, 72 (1996).
- [34] L. L. Daemen, L. N. Bulaevskii, M. P. Maley and J. Y. Coulter, Phys. Rev. Lett. **70**, 1167 (1993).
- [35] D. Ertaş and D. R. Nelson, Physica C **272**, 79 (1996); T. Giamarchi and P. L. Doussal, Phys. Rev. B **55**, 6577 (1997); V. Vinokur, B. Khaykovich, E. Zeldov, M. Konczykowski, R. A. Doyle and P. Kes, Physica C **295**, 209 (1998); J. Kierfeld, Physica C **300**, 171 (1998).
- [36] D. Giller, A. Shaulov, Y. Yeshurun and J. Giapintzakis, Phys. Rev. B **60**, 106 (1999).

- [37] V. Hardy, A. Wahl, A. Ruyter, A. Maignan, C. Martin, L. Coudrier, J. Provost, Ch. Simon, *Physica C* **232**, 347 (1994); K. Shibata, T. Nishizaki, T. Sasaki and N. Kobayashi, *Phys. Rev. B* **66**, 214518 (2002); T. Masui, Y. Takano, K. Yoshida, K. Kajita and S. Tajima, *Physica C* **412-414** 515 (2004).
- [38] V. F. Correa, J. A. Herbsommer, E. E. Kaul, F. de la Cruz and G. Nieva, *Phys. Rev. B* **63**, 092502 (2001).
- [39] A. I. Larkin and Yu. N. Ovchinnikov, *J. Low Temp. Phys.* **34**, 409 (1979).
- [40] C. P. Bean, *Rev. Mod. Phys.* **36**, 31 (1964).
- [41] N. Jenkins (private communication).
- [42] M. Nideröst, R. Frassanito, M. Saalfrank, A. C. Mota, G. Blatter, V. N. Zavaritsky, T. W. Li, and P. H. Kes, *Phys. Rev. Lett.* **81**, 3231 (1998).
- [43] Ø. Fischer, M. Kugler, I. Maggio-Aprile, C. Berthod, and Ch. Renner, *Rev. Mod. Phys.* **79**, 353 (2007), and references therein.
- [44] J. L. Tallon, C. Bernhard, U. Binniger, A. Hofer, G. V. M. Williams, E. J. Ansaldo, J. I. Budnick, and Ch. Niedermayer, *Phys. Rev. Lett.* **74**, 1008 (1995).
- [45] N. Clayton, N. Musolino, E. Giannini, V. Garnier and R. Flükiger, *Supercond. Sci. Technol.* **17**, S563 (2004).
- [46] D. Darminto, M. Diantoro, I. M. Sutjahja, A. A. Nugroho, W. Loeksmanto, and M. O. Tjia, *Physica C* **378-381**, 479 (2002).
- [47] D. Darminto, M. O. Tjia, A. A. Nugroho, A. A. Menovsky, J. Shimoyama, and K. Kishio, *Physica C* **357-360**, 617 (2001).
- [48] N. Musolino, N. Clayton, and R. Flükiger, *Physica C* **417**, 40 (2004).
- [49] Y. Nakayama, T. Motohashi, K. Otschi, J. Shimoyama, K. Kitazawa, K. Kishio, M. Konczykowski, and N. Chikumoto, *Phys. Rev. B* **62**, 1452 (2000).
- [50] V. J. Emery and S. A. Kivelson, *Nature* **374**, 434 (2002).

Fig.1, Piriou et al., PRB

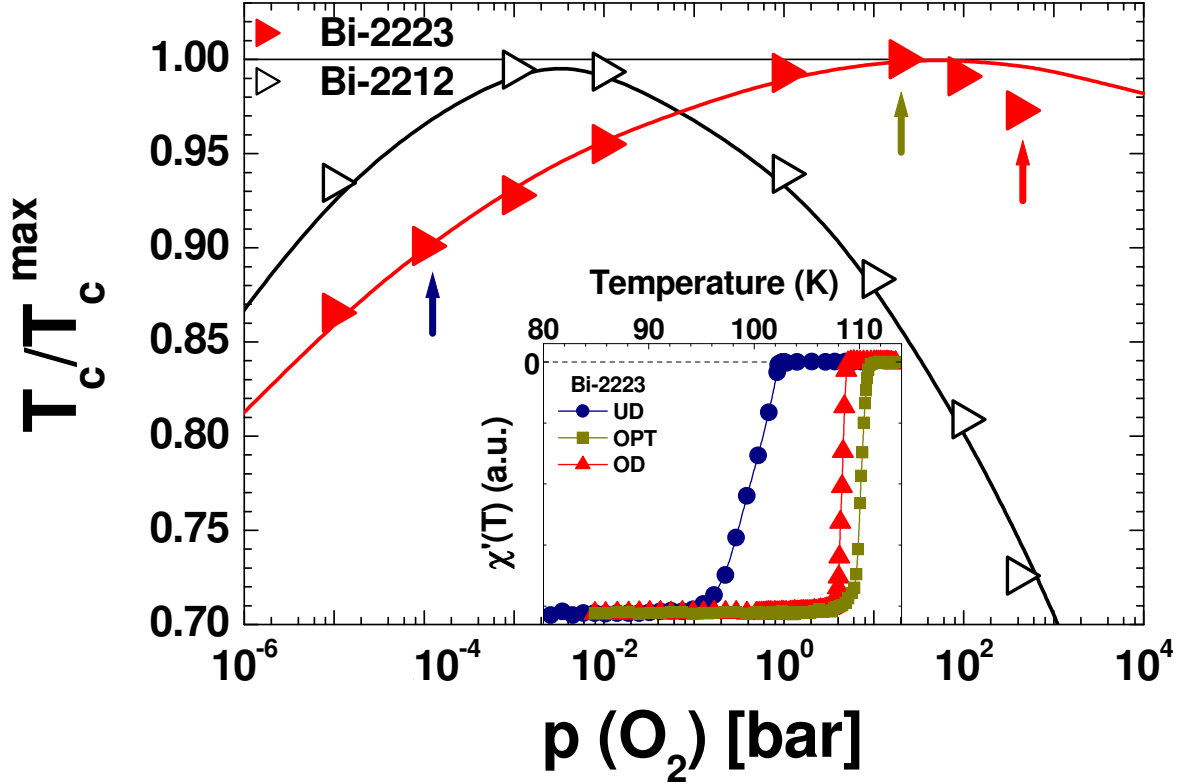


FIG. 1: Normalized critical temperature as a function of post-annealing oxygen pressure $p(O_2)$ for Bi-2223 and Bi-2212. The maximum values of critical temperatures are (90.5 ± 0.5) and (110.5 ± 0.5) K for Bi-2212 and Bi-2223, respectively. The lines are fits of the data with the universal relation $T_c = T_c^{\max}(1 - 82.6(\delta - 0.27)^2)$ [25, 26, 27] with $\delta = 0.011 \ln p(O_2) + 0.3$ [27] for Bi-2212 and $\delta = 0.006 \ln p(O_2) + 0.26$ for Bi-2223. Every point in $p(O_2)$ corresponds to at least ten samples and the size of the points includes the dispersion in critical temperature. The arrows indicate the different doping levels tuned in the sample used to study the doping-dependence of the Bi-2223 vortex phase diagram. Insert: Real part of the susceptibility as a function of temperature for the same sample of Bi-2223 in the UD ($T_c(100 \pm 2)$ K), OPT ($T_c(110.5 \pm 0.5)$ K) and OD ($T_c(107 \pm 0.5)$ K) regimes. The $\chi'(T)$ measurements were performed with an AC field of 0.1 Oe in magnitude and 970 Hz in frequency.

Fig.2, Piriou et al., PRB

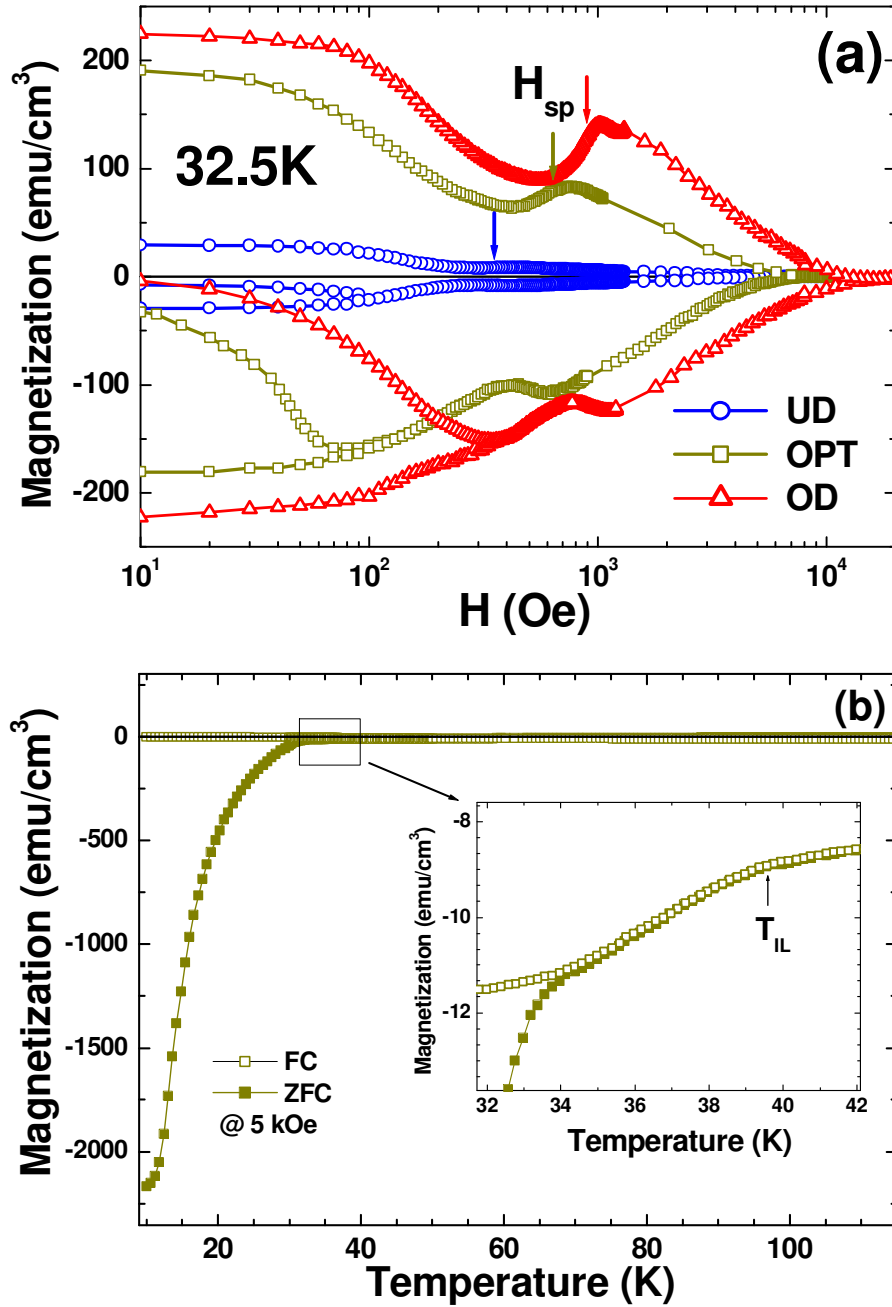


FIG. 2: (a) Magnetization loops at 32.5 K for the same sample for UD ($T_c = (100 \pm 2)$ K), OPT ($T_c = (110.5 \pm 0.5)$ K) and OD ($T_c = (107.0 \pm 0.5)$ K) oxygen concentrations. The second peak field $H_{SP}(T)$ is indicated with arrows. (b) Field-cooling (FC) and Zero-field-cooling (ZFC) magnetization measurements for the OPT regime at an applied field of 5 kOe. The onset-temperature of the irreversible magnetic behavior at 5 kOe, T_{IL} , is indicated.

Fig. 3, Piriou et al., PRB

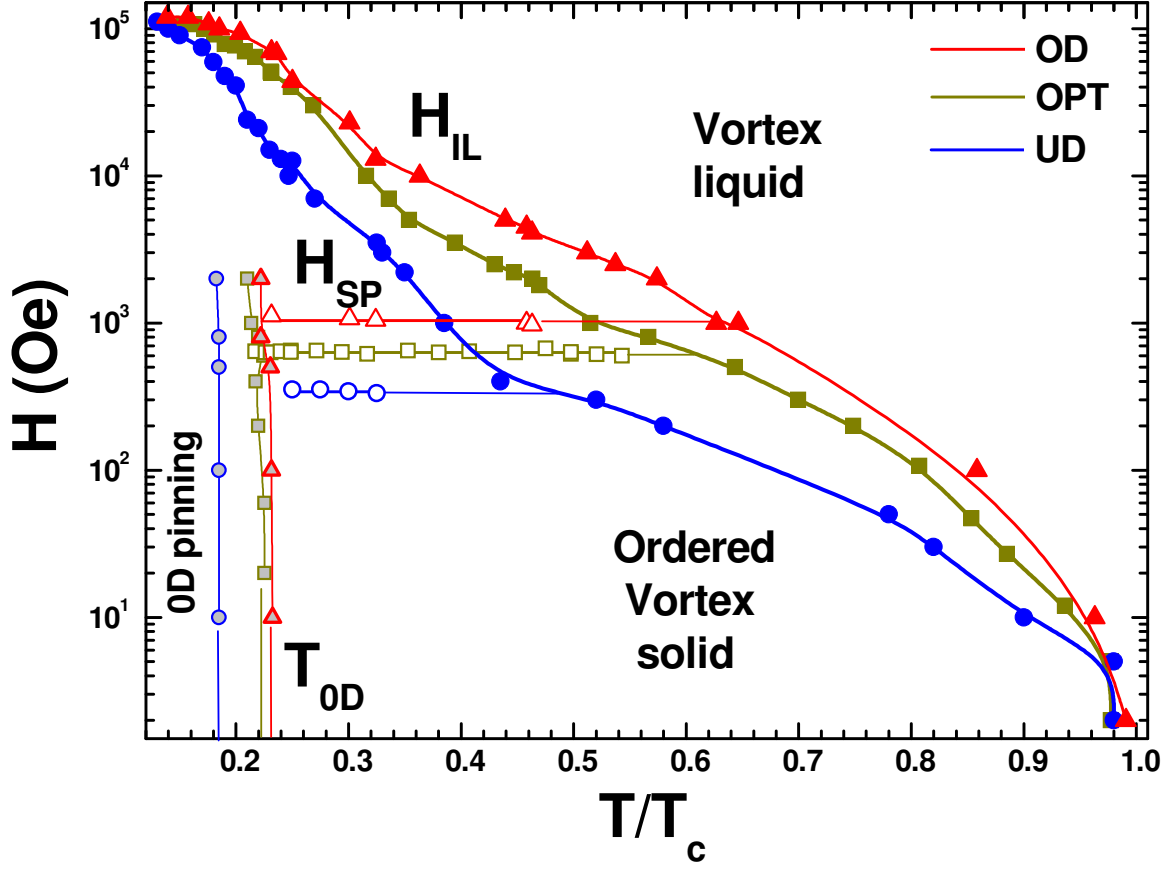


FIG. 3: Vortex phase diagram for the same sample in UD (\circ), OPT (\square) and extremely OD (\triangle) regimes. The irreversibility, $H_{IL}(T)$ (full symbols), second peak $H_{SP}(T)$ (open symbols) and zero-dimensional pinning $T_{0D}(H)$ (gray-filled symbols) lines are shown. The error in magnetic field and temperature of the measured points is included in their size.

Fig.4, Piriou et al., PRB

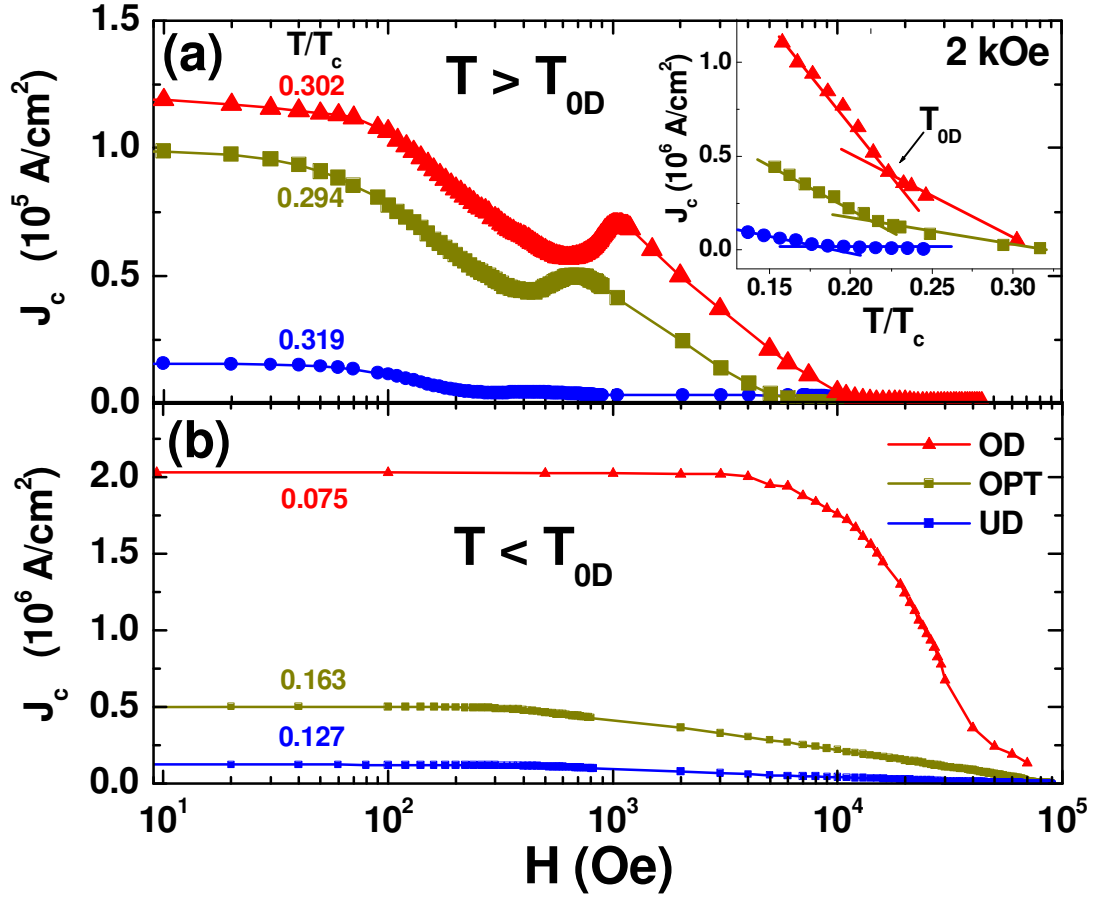


FIG. 4: Critical current density as a function of magnetic field , $J_c(H)$, for (a) $T > T_{0D}$ and (b) $T < T_{0D}$. Insert: Curves of J_c vs. reduced temperature obtained from the width of the magnetization loop at 40 Oe (see text). The arrows indicate the kink in J_c considered as the temperature T_{0D} at which the zero-dimensional pinning sets in.

Fig. 5, Piriou et al., PRB

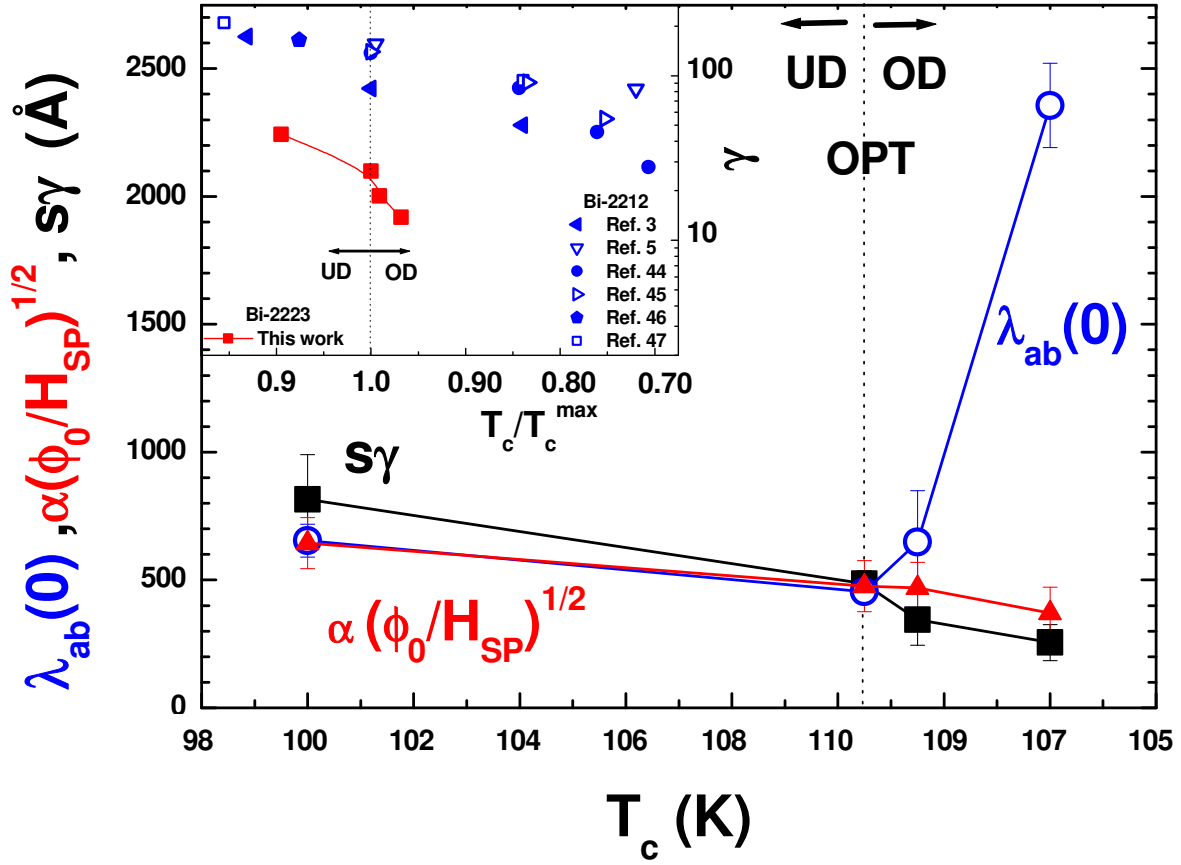


FIG. 5: Evolution of the in-plane penetration depth, $\lambda_{ab}(0)$, the anisotropy, $s\gamma$, and the second-peak field, $\propto \sqrt{\Phi_0/H_{SP}}$, for the UD, OPT and OD regimes of Bi-2223. Inset: Electronic anisotropy as a function of T_c/T_c^{max} for our Bi-2223 sample and values reported in the literature for numerous Bi-2212 samples [3, 5, 46, 47, 48, 49].